Chinese Journal of
POLYMER SCIENCE

RESEARCH ARTICLE

https://doi.org/10.1007/s10118-025-3546-9
Chinese J. Polym. Sci. **2026**, *44*, 857–868

Reentrant Phase Behavior in Diblock Copolymer AB/Homopolymer C Blends: A Combined Effect of Solvent Selectivity and Block Interactions

Zhi-Yao Liu[a*], Hui Wang[a], Hong-Xia Bu[a], Juan Wang[a], Bao-Hui Li[b], and Lu-Lu Liu[c]

[a] *School of Physics and Electronic Engineering, Qilu Normal University, Jinan 250200, China*
[b] *Key Laboratory of Weak-Light Nonlinear Photonics, Ministry of Education, School of Physics, Nankai University, Tianjin 300071, China*
[c] *Department of Thermal Engineering, Shandong Jianzhu University, Jinan 250101, China*

Electronic Supplementary Information

Abstract We investigated the phase behavior of diblock copolymer AB/homopolymer C blends in concentrated aqueous solutions using a simulated annealing method. Phase diagrams were constructed as a function of the concentration of all polymers (Φ) and the volume fraction of homopolymer (f_C). Rich phase transition sequences were observed, especially reentrant phase transitions, such as lamellae → inverted cylinders → gyroids → lamellae → disorder, for a given Φ with increasing f_C. By analyzing the variations in the average contact numbers between different components and the effective volume fractions of B-domains, we elucidated the mechanisms of the reentrant phase transitions. We found that the strong attraction between B and C leads to the swelling of B-domains upon addition of homopolymer. Concurrently, the solvent preferentially swells the A-domains over the B+C-domains. The competing swelling effects of the solvent and homopolymer on the A-domains and B-domains, respectively, triggered the reentrant phase behavior in the symmetric AB copolymer system upon addition of homopolymer.

Keywords Simulated annealing; Diblock copolymer; Homopolymer; Blend; Solution

Citation: Liu, Z. Y.; Wang, H.; Bu, H. X.; Wang, J.; Li, B. H.; Liu, L. L. Reentrant phase behavior in diblock copolymer AB/homopolymer C blends: a combined effect of solvent selectivity and block interactions. *Chinese J. Polym. Sci.* **2026**, *44*, 857–868.

INTRODUCTION

Block copolymers (BCPs) have great potential for applications in nanotechnology,[1–3] including drug delivery,[4,5] nanolithography,[6,7] and energy conversion.[8,9] This is due to their ability to spontaneously self-assemble into microphase separated domains with uniform size ranging from several to tens of nanometers. The simplest BCPs, diblock copolymers[10–13] form lamellae, hexagonally packed cylinders, body-centered-cubic spheres and the gyroid structure. Their phase behavior can be controlled by the degree of segregation χN (where χ is the Flory-Huggins interaction parameter and N is the degree of polymerization) and the volume fractions of the blocks. Notably, traditional phase behaviors mostly exhibit unidirectional phase transition sequences. In contrast, reentrant phase transitions (a special phase transition where a phase reappears with the continuous variation of an external parameter) offer new possibilities for the diversified regulation of BCP phase structures. Investigations into reentrant phase transitions not only possess significant fundamental scientific merit by revealing the complex equilibrium of competitive interactions,[14–16] but also offer substantial practical potential in materials science, biomedicine, and industrial applications. For instance, relevant advances have been reported in the design and stability optimization of semiconductor materials,[17] the formation of intracellular membraneless organelles,[18] and the design of interactive and adaptive soft materials.[19]Adding solvents is an effective and economical method to regulate BCP morphologies.[20–23] Currently, the solution self-assembly of both amphiphilic[24–27] and double-hydrophilic[28–33] diblock copolymers has been systematically investigated. Among these, studies on double-hydrophilic diblock copolymers solutions are particularly noteworthy: for a single copolymer, rich phase transition sequences—with reentrant phase transitions as a typical example—can be observed by reducing the polymer concentration.[31–33] For instance, Blanazs *et al.*[31] observed a sequence of phase transitions from lamellae → cylinders → lamellae → disordered phase by reducing the polymer concentration. Similarly, Wu *et al.*[33] predicted *via* simulated annealing that the system exhibits a more complex reentrant phase sequence (lamellae → gyroids → cylinders → gyroids → lamellae → disorder) with decreasing concentration.

* Corresponding author, E-mail: liuzhiyaonku@163.com
Received November 26, 2025; Accepted January 5, 2026; Published online February 6, 2026

Besides solvent modulation, blending is another efficient and economical approach to obtain new materials, as the final products can combine and enhance the properties of their components.[34–37] In polymer systems containing BCPs, a typical example is the blend of diblock copolymer AB/homopolymer C (hereafter referred to as AB/C blends).[38–49] For high molecular weight polymers, mixing entropy is greatly diminished, making miscibility largely dependent on the interactions between various monomer types. This fact dictates that polymer blends often tend to phase separate macroscopically. To inhibit the macrophase separation, the simplest and most investigated possibility is that the A and B blocks are immiscible, whereas C is miscible (*via* ion-dipole, π-π interactions, or hydrogen bonding) with one block but is immiscible with the other block. For example, Matsushita *et al*.[38–40] systematically studied the blends of diblock copolymer polystyrene-*b*-poly(2-vinylpyridine) (PS-*b*-P2VP) and poly(4-vinylphenol) (PVPh) homopolymer, where PVPh is miscible with the P2VP block through the hydrogen bonding interaction, but is immiscible with PS. The researchers found that all blends displayed well-ordered nano-phase separation, independent of the molecular weight of the polymers and the quantity of homopolymer. Therefore, in the AB/C blends, hydrogen bonding plays a crucial and decisive role in the self-assembled structure, which can inhibit macroscopic phase separation. Dehghan *et al*.[41] used self-consistent field theory (SCFT) with an attractive-interaction model to investigate the phase behaviors of AB/C blends. In the strong hydrogen-bonding region, they obtained order-order transitions from lamellae to cylinders and, finally, to spheres upon increasing the volume fraction of homopolymer.

In contrast to amphiphilic and double-hydrophilic diblock copolymers, the phase behaviors of AB/C blends in solution are poorly understood. Previous research on AB/C blends in solution has primarily focused on vesicle or micelle formation at low polymer concentrations.[50,51] To the best of our knowledge, there are currently only a few reports on the phase behaviors of AB/C blends in concentrated solutions.[52–55] For instance, Liu *et al*.[52] reported a facile route to prepare asymmetric mesoporous carbon microparticles by neutral interface-guided 3D-confined self-assembly of block copolymer/homopolymer blends; our team previously studied the solvent-induced compatibilization effects in AB/C blends by selecting specific solvents to modulate the interfacial interactions between polymers;[53] Tan *et al*.[54] experimentally investigated a polystyrene-*b*-poly(2-vinyl pyridine) (PS-*b*-P2VP)/molybdophosphate ($H_3PW_{12}O_{40}$, PW) blended system, identifying not only lamellae, cylinders, and spheres but also inverted cylindrical phases; Moreover, a halogen-bond driven confined-assembly pathway to enable phase transitions was reported.[55] An order-to-order morphology transition sequence: spheres → cylinders → lamellae → inverted cylinders was obtained from polystyrene-*b*-poly(4-vinyl pyridine) (PS-*b*-P4VP)/poly(3-(2,3,5,6-tetrafluoro-4-iodophenoxy) propyl acrylate (PTFIPA) blends by tuning the PTFIPA content and choice of surfactant. However, despite such progress, a comprehensive understanding of AB/C solution systems' phase behavior in concentrated solutions remains limited: critically, reentrant phase transitions have not yet been reported in this system. Moreover, previous work has predominantly focused on single-variable regulation (*e.g.*, the volume fraction of homopolymer f_C), failing to reveal the synergistic effects between f_C and multiple interaction parameters (such as Φ, B-S, B-C, and A-B interactions) on the nonlinear modulation mechanisms of phase behavior—limitations that severely constrain the application potential of these systems in the precision fabrication of functional materials.

In this study, we employed a simulated annealing technique to explore the phase behavior of AB/C triple-hydrophilic block copolymers in concentrated solutions. A variety of phase diagrams was constructed as a function of polymer concentration Φ and the volume fraction of homopolymer f_C, as well as f_C and B-C interaction, f_C and B-solvent interaction, and f_C and A-B interaction. Special attention is paid to the inverted phases and reentrant phase transitions emerging during phase transformations. The mechanisms of phase transitions upon dilution are elucidated by analyzing the variations of the effective volume fractions and the average contact numbers, thereby bridging the theoretical gaps in this field.

MODEL AND METHOD

Our simulations were performed using the simulated annealing method and the "single-site bond fluctuation" model.[56,57] The simulated annealing method is a well-known procedure for obtaining the lowest energy "ground states" of disordered systems.[58] The combination of lattice models and simulated annealing methods has been demonstrated to be an effective approach for studying the self-assembly of block copolymers in solution and under confinement.[59,60] In this section, the model and simulation algorithm are reviewed briefly and a detailed description could be found elsewhere.[61–64]

The simulations were performed on a model system that was embedded in a simple cubic lattice of volume $V = L^3$ with L being the number of lattice layer in each direction. Periodic boundary conditions are applied in all 3 directions. In our simulations, the volume of the simulation box was fixed at $V = 24 \times 24 \times 24$ for all systems; however, larger simulation boxes with sizes $36 \times 36 \times 36$ and $48 \times 48 \times 48$, were also employed to verify the reproducibility of the structures in typical regions of a phase diagram. Furthermore, when a gyroid, perforated lamellar, or disordered structure was formed, the simulation box size was varied continuously within the range of L=24–52 to identify the morphology. Each segment occupies one lattice site and two consecutive segments are connected by bonds that can adopt a length of 1 or $\sqrt{2}$ in lattice spacing, and hence each lattice site has 18 nearest neighbor sites. The polymers are modeled to be self- and mutual-avoiding random walks, and thus, no two or more segments can occupy the same site simultaneously. The system is composed of three components: diblock copolymer, homopolymer, and solvent. Each diblock copolymer chain has N_A A-monomers and N_B B-monomers. The homopolymer is composed of N_C C-monomers. There are n_{AB} copolymer chains and n_C homopolymer chains in the systems. The volume fraction of the homopolymer is f_C, $f_C = V_C/(V_A + V_B + V_C)$; $V_A = n_{AB} \times N_A$; $V_B = n_{AB} \times N_B$; $V_C = n_C \times N_C$. The total monomer concentration of both diblock copolymer and homopolymer is defined as Φ, $\Phi = (V_A + V_B + V_C)/V$. The initial state is generated by putting

https://doi.org/10.1007/s10118-025-3546-9

an array of polymer chains onto the lattice. The remaining empty sites are assigned to solvent molecules. The energy of the system is calculated by taking account of the pair interactions between different species on two nearest neighbor lattice sites. Interaction energy $E_{ij} = \varepsilon_{ij}k_BT_{ref}$ is assigned for each pair of components i and j, where i, j = A, B, C and S (solvent); ε_{ij} is the reduced interaction energy; k_B is the Boltzmann constant; T_{ref} is a reference temperature. It is assumed that ε_{ii} =0, with i = A, B, C, and S.

To elucidate the mechanism of phase transitions in the system with varying polymer concentration and homopolymer volume fraction, we calculated the average contact numbers between different species and the effective volume fraction variations of B-domains (f_{eB}), whose calculation method is similar to previous ones.[33,65] There are four species in contact with each monomer: A monomer, B monomer, C monomer, and solvent (S). The average contact number for each A monomer with B monomer is defined as n_{AB}. Similarly, the average contact number between the other monomers is defined in the same way. The effective volume fraction of B-domains (f_{eB}) is defined as the ratio of the number of the lattice sites occupied by B-domains ($N_{B\text{-}d}$) to the number of total lattice sites. $N_{B\text{-}d}$ equals the sum of the number of B monomers, the number of solvent molecules belonging to the B-domains, and the number of homopolymers belonging to the B-domains. Classification rules for homopolymers: (1) If a homopolymer only contacts B-monomers and does not contact A-monomers, it is determined to be located within the B-domains; (2) If a homopolymer contacts both A-monomers and B-monomers, half of the homopolymer is attributed to the B-domains in a lamellar structure; the homopolymer is attributed to the B-domains in a non-lamellar structure. Classification rules for solvent molecules: (1) if a solvent molecule only contacts B-monomers and does not contact A-monomers, it is determined to be located within the B-domains; (2) If a solvent molecule contacts both A-monomers and B-monomers: in a lamellar structure, half of the solvent molecule is attributed to the B-domains; if the B-domains is the dispersed phase in a non-lamellar structure, count the number of A-monomers and B-monomers around the solvent molecule, and compare the two numbers, if there are more B-monomers around, the solvent molecule belongs to the B-domains. It should be mentioned that at a given f_{eB} value, the effective volume fraction of the A-domains is given by $f_{eA} = 1 - f_{eB}$. It should be noted that the above allocation rule is based on different morphological characteristics and the interaction parameters. In the lamellar phase, when solvent or homopolymer is distributed at the interlayer interface, it is the most reasonable treatment to allocate half of them to each of the two adjacent layers. For non-lamellar phases: due to its strong affinity with B and repulsion against A, homopolymer C usually forms a mixed domain with B. Thus, when it is at the interface, it is attributed to the B-domains. For solvents, since their attraction to A and B is equivalent, when they are at the interface, it is more reasonable to count and compare the number of adjacent A and B monomers, and attribute the solvent to the domain with the larger number of monomers. This allocation rule is consistent with previous studies.[65]

RESULTS AND DISCUSSION

For the studied system of diblock copolymers AB/homopolymer C blends in concentrated aqueous solutions, the phase space is huge, with 5 independent compositional parameters (N_A, N_B, N_C, f_C, Φ) and 6 inter-segment interaction parameters (ε_{AB}, ε_{BC}, ε_{AC}, ε_{AS}, ε_{BS}, ε_{CS}), totaling 11 parameters. To simplify the investigation, we fixed N_C=2 and typically set N_A=N_B=6. Only when investigating the effect of A-B asymmetry on the system were N_A and N_B adjusted specifically to 9 and 3, respectively. The reason for choosing these chain lengths is that in simulations of AB diblock copolymers, the simplified chain length notation such as A_nB_{12-n} is commonly used.[25,33] The chain length ratio of block copolymer to homopolymer in this study is 6:1, which is consistent with the molecular weight ratio range in experimental systems. For example, when investigating the AB/C blending system, the Matsushita group[38,40] covered a molecular weight ratio range of (3–10):1 between poly(styrene-*b*-2-vinylpyridine) diblock copolymer and poly(4-hydroxystyrene)s; Additionally, our previous research[53] has also examined the effects of various ratios such as A_6B_6/C_2, A_6B_6/C_4, and A_6B_6/C_6 on the system behavior. In this study, we focus on investigating the effects of parameters such as the homopolymer volume fraction, solvent selectivity, and total polymer concentration on the self-assembly of the system. Thus, only two cases, A_6B_6/C_2 and A_9B_3/C_2, were investigated. First, we studied the condition where A- and B-blocks are completely symmetric in the absence of added homopolymer, with the interactions between A and S, and between B and S set as the same attractive interaction, and ε_{AS}=ε_{BS}=−2.0. This enables us to isolate the effect of f_C on the phase structure of the system. To inhibit the macrophase separation, we set the A-and B-blocks to be immiscible (ε_{AB}=4.0), whereas C is miscible with B-blocks (ε_{BC}=−4.0) but is immiscible with A-blocks (ε_{AC}=2.0). This parameter set models scenarios in experiments involving non-covalent interactions such as ion-dipole, π-π stacking, or hydrogen bonding. Furthermore, we separately studied the effects of varying the degree of incompatibility between A- and B-blocks (ε_{AB}) and the strength of non-covalent interactions (ε_{BC}) on the system. For the solvent, we initially examined the case where the solvent exhibits the same attractive interaction with both A-and B-blocks, *i.e.*, $\varepsilon_{AS} = \varepsilon_{BS} - 2.0$. Subsequently, we studied the impact of changing the ε_{BS} on the system. The solvent interaction for C was set to ε_{CS}=−0.2. Based on the aforementioned parameters, we plotted phase diagrams as a function of the polymer concentration Φ and the volume fraction of homopolymer f_C (Fig. 1a). The mechanism of phase transitions was elucidated through analysis of the average contact numbers between different species (Fig. 2 and Figs. S1 and S2 in the electronic supplementary information, ESI) and effective volume fraction variations (Fig. 3). Subsequently, we investigated the effects of interaction parameters on the system's phase structure, generating phase diagrams as a function of f_C and B-C interaction (Fig. 4a), f_C and B-solvent interaction (Fig. 5a), and f_C and A-B interaction (Fig. 6a). The underlying mechanisms were further examined through corresponding variations in effective volume fractions (Figs. 4b, 5b and 6b). We reported the simulation results for asymmetric diblock copolymer/homopolymer A_9B_3/C_2 blends (Fig. 7) with comparative analysis against symmetric A_6B_6/C_2 blends. Finally, the distribution of homopolymer and solvent molecules in lamellae is presented as a

https://doi.org/10.1007/s10118-025-3546-9

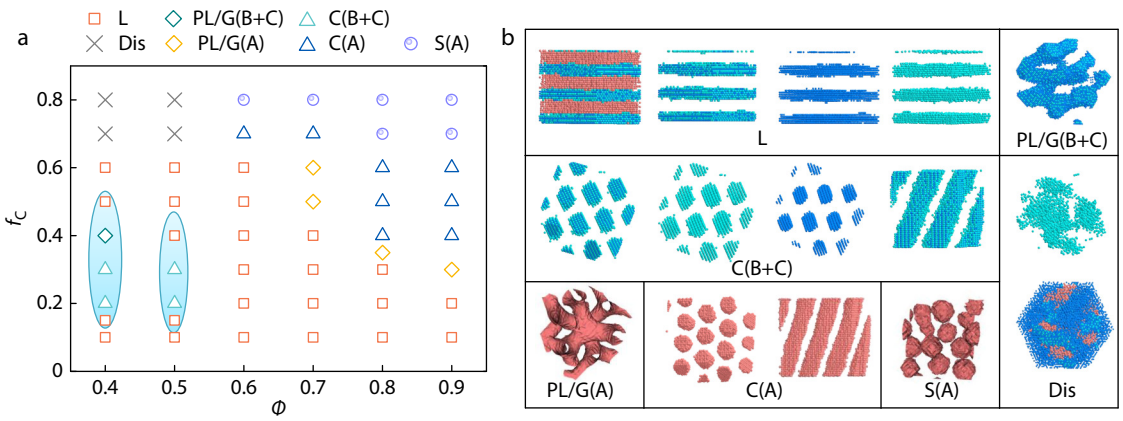

Fig. 1 (a) Phase diagram in the volume fraction of homopolymer (f_C) and the concentration (Φ) space for A_6B_6/C_2 blends in solutions with ε_{AB}=4.0, ε_{BC}=−4.0, ε_{AC}=2.0, ε_{AS}=−2.0, ε_{BS}=−2.0, ε_{CS}=−0.2; (b) Typical snapshots for the self-assembled structures. In the legend, L: lamellae, PL/G: perforated lamellae/gyroids, C: hexagonally-packed cylinders, S: spheres, Dis: disordered phase. A phase labeled with "A" or "B+C" means that the phase is formed by the A-domains or B+C-domains. Color scheme in the snapshots: A (red), B (green), C (blue).

function of f_C (Figs. 8 and 9).

Effects of Homopolymer Fraction and Polymer Concentration

Fig. 1(a) presents the phase diagram in the parameter space specified by the polymer concentration Φ and the volume fraction of homopolymer f_C with ε_{AB}=4.0, ε_{BC}=−4.0, ε_{AC}=2.0, ε_{AS}=−2.0, ε_{BS}=−2.0, ε_{CS}=−0.2. The typical snapshots for the phases that occurred are shown in Fig. 1(b). In the lamellae (L) structure, one layer is composed of A-blocks and solvent, whereas adjacent layers are formed by the mixture of B-blocks, homopolymer C and solvent, with the layers alternating in a stacked arrangement. The symbols G(A), C(A) and S(A) denote respectively the gyroid phase, hexagonally packed cylinders, and spherical phase formed by the A blocks and solvent, and the mixture of B-blocks, homopolymer C and solvent forms the matrix. The PL/G(B+C) and C(B+C) are the perforated lamellae or gyroid structure and the hexagonally packed cylinders, respectively, formed by the mixture of B-blocks, homopolymer C and solvent, with the A-blocks and solvent forming the matrix. These structures were called inverted phases. In this work, the inverted phase is defined using the melt state of symmetric diblock copolymer/homopolymer blends (*i.e.*, zero solvent content) as the initial reference system. Previous study[41] showed that when homopolymer C exhibits strong interactions with B-blocks of the diblock copolymer while repelling A-blocks, the addition of homopolymer C into the melt system leads to the incorporation of C into the B-domains. At this point, the total volume fraction of B- and C-domains exceeds 0.5, thus forming the matrix, whereas A-blocks self-assemble into ordered phase structures. In contrast, upon introducing solvents into the system in our study, an opposite phase behavior can be observed: the ordered phase is formed by the mixture of B-blocks, homopolymer C, and solvent, with the A-blocks and solvent forming the matrix. Such inverted phases have also been reported in other relevant studies.[55,65,66] In addition, the structure Dis (disorder phase) refers to a state where the system fails to form regular ordered phases.

In Fig. 1(a), the lamellae phase can always be observed when f_C=0.1 regardless of the polymer concentration. It is noted that the bulk phase of the A_6B_6 copolymer is lamellar phase.[13] It is worth noting that at low polymer concentrations of Φ=0.4 and 0.5, reentrant phase transitions with the sequences of L → C(B+C) → PL/G(B+C) → L → Dis, and of L → C(B+C) → L → Dis, and these inverted phases are obtained, respectively, with increasing f_C. At high polymer concentrations of Φ≥0.6, phase transitions with the sequence L → G(A) → C(A) → S(A) are obtained, and the G(A) phase is not necessarily observed due to its narrow phase region. These morphological sequences agree with the phase behavior predicted by using the self-consistent field theory for AB/C blends with equal-sized A and B blocks and B/C strongly attraction in bulk and experimental observations.[41–49]

The reentrant phase transitions and the occurrence of inverted phases at low concentrations are both unusual and interesting. In order to understand this unusual phenomenon and the differences in the self-assembly behavior of the system under high polymer concentrations and low polymer concentrations, we calculated the average contact numbers between different species (Fig. 2 and Figs. S1 and S2 in ESI) and effective volume fraction of B domains (f_{eB}) (Fig. 3). At high polymer concentrations Φ=0.9 (Fig. 2), n_{AS} increases from 2 to 9; n_{BS} decreases from 2 to 1; n_{CS} is very small (close to 0) with increasing f_C. This indicates that as the volume fraction of the homopolymer increases, the solvent prefers staying in the A-domains rather than the B+C-domains. This observation is consistent with the parameter settings where the solvent is strongly attractive to both blocks of the copolymer (A and B), but less attractive to the homopolymer (C). It should also be noted that n_{BC} increases rapidly, reaching the value of about 16, while the value of n_{AC} is quite small with increasing f_C. The results indicate that homopolymer incorporation induces preferential swelling in the B-domains over the A-domains. It is in reasonable agreement with the parameters in the system where the B/C interaction is the strongest, while the interaction between A and C is repulsion. However, the attractions between B and C are dominant at high polymer concentrations, whereas the effect of the solvent is relatively smaller, since the solvent content is minimal under this condition. The phase behavior of the system resembles that of an AB/C melt system, leading to L → G(A) → C(A) → S(A)

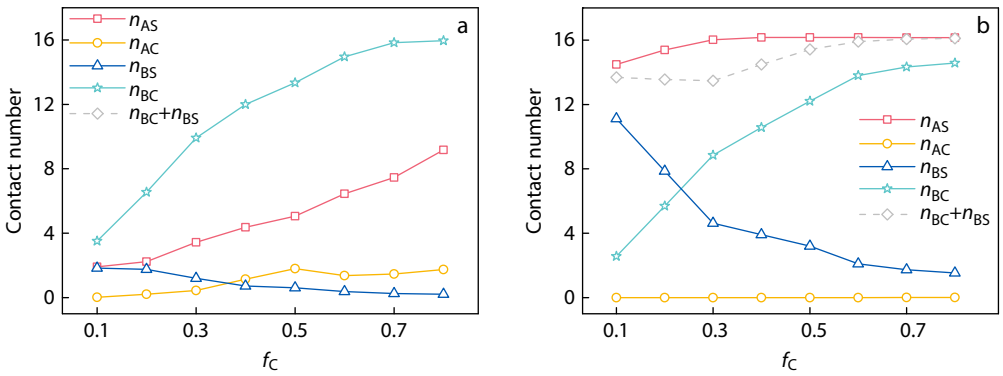

Fig. 2 Variations of the average contact numbers with the volume fraction of homopolymer (f_C) at polymer concentration (a) Φ=0.9 and (b) Φ=0.4 for A_6B_6/C_2 blends in solutions with ε_{AB}=4.0, ε_{BC}=−4.0, ε_{AC}=2.0, ε_{AS}=−2.0, ε_{BS}=−2.0, ε_{CS}=−0.2.

transition.

At low polymer concentrations Φ=0.4, *i.e.*, when there is a large amount of solvent, the phase behavior depends not only on the homopolymer addition but also on the solvent selectivity. As shown in Fig. 2(b), the n_{BC} increases rapidly, reaches the value of about 14 with increasing f_C. The value of n_{AC} is quite small, slightly greater than zero. Additionally, upon increasing the f_C, n_{AS} increases from 14 to its maximum 16 and finally keeps the maximum value, but n_{BS} decreases rapidly from 11 to 1 and n_{CS} increases from 4 to 10. It is noted that when homopolymer is added, the solvent molecules mainly swell the A-domains rather than B+C-domains, *e.g.*, n_{AS}=14.5, n_{BS}=11.1, n_{CS}=3.3 at f_C=0.1; n_{AS}=15.4, n_{BS}=7.9, n_{CS}=2.2 at f_C=0.2; n_{AS}=16.0, n_{BS}=4.6, n_{CS}=2.7 at f_C=0.3. As the amount of homopolymer increases, n_{AS} peaks at f_C=0.3 and remains constant thereafter. The total contact number for each monomer should be the same as the number of the nearest neighbors, which is 18 in our model. Since there are 2 bonded monomers (the chain end monomer has one bonded monomer) for each monomer, about 16 is the maximum value that n_{AS} can reach theoretically. As the value of f_C increases, n_{AS} remains at its maximum for f_C≥0.3, while n_{BS} continuously decreases and n_{CS} gradually increases (Fig. S2 in ESI).

To establish a link between the phase transition behaviors observed in the phase diagrams (Fig. 1a) and the underlying structural mechanisms, we analyzed the effective volume fraction of B-domains (f_{eB}) as a key quantitative indicator, whose calculation methodology has been detailed in **MODEL AND METHOD** section. Specifically, f_{eB} quantifies the relative swollen volume of B-rich regions, integrating contributions from B-blocks, associated homopolymer C, and solvent molecules within these domains—thus serving as a direct bridge between component interactions and phase morphologies. It should be noted that in the ordered phases (L, C(B+C), PL/G(B+C), L, G(A), C(A), S(A)), B-blocks and homopolymer are homogeneously distributed even when the value of f_C is relatively large. Their phase structures have been presented in the description of Fig. 1(b). In the disordered phase (Dis), in addition to the regions where the homopolymer is homogeneously distributed with B-blocks, another portion of homopolymer forms separate regions, resulting in macroscopic phase separation. These separate regions are also counted as B-domains in the calculation.

Fig. 3 presents the variation of f_{eB} with the volume fraction of homopolymer (f_C) for A_6B_6/C_2 blends, which corresponds to the parameters in Fig. 1(a). In the L phase regions, f_{eB} approaches 0.5, which is consistent with the volume fraction of the lamellar phase in the pure diblock copolymer. This confirms that our calculation for f_{eB} is correct. Interestingly, we found that nonmonotonic variation in the effective volume fraction which corresponds to the reentrant phase transitions. Specifically, for Φ=0.4–0.5, f_{eB} first decreases, then reaches a minimum value, and finally increases with increasing f_C. This trend was exemplified at Φ=0.4 (Fig. 3), where f_{eB} progressively decreases for f_C<0.3, attains a minimum of 0.40 at f_C=0.3, and then increases for 0.3<f_C<0.8 with increasing f_C. This nonmonotonic behavior corresponds to the phase transition sequence of L → C(B+C) → PL/G(B+C) → L. At the same f_C<0.7, the value of f_{eB} at Φ=0.5 is slightly larger than that at Φ=0.4. On the other hand, when Φ≥0.6, f_{eB} increases monotonically with increasing f_C, in stark contrast to the nonmonotonic variation features when Φ = 0.4 and 0.5. This is consistent with the phase transition sequence of L → G(A) → C(A) → S(A) shown in the phase diagram in Fig. 1(a). As is well-known, the phase transitions of BCPs follow the principle of total free energy minimization: in the low-curvature lamellar phase, chain segments of both components can fully extend within the continuous domains, resulting in minimal loss of conformational entropy. Despite the interfacial area is relatively large, the advantage of chain conformational entropy dominates the reduction in total free energy, thus rendering the lamellar phase the thermodynamically stable phase at symmetric composition (f=0.5). With the increases of chain asymmetry, the low-curvature structure causes excessive chain stretching due to the mismatch in volume fractions, leading to a drastic increase in conformational entropy loss; at this stage, the system tends to form high-curvature structures (*e.g.*, cylinders, spheres). The transition of phase structures is essentially the thermodynamically optimal state for the system to achieve the balance between "interfacial free energy and conformational entropy" under different curvature conditions. For the bulk diblock copolymers, this regularity has been fully verified by phase diagram results from self-consistent field theory (SCFT) calculations and Monte Carlo (MC) simulations. As the chain asymmetry of the copolymer increases (*i.e.*, f_A=0.5 → f_A=0 or f_A=0.5 → f_A=1), the phase-separated structure gradually evolves into morphologies with higher curva-

https://doi.org/10.1007/s10118-025-3546-9

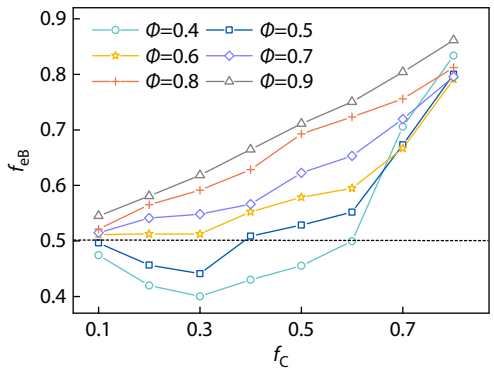

Fig. 3 Variation of the effective volume fractions of B-domains (f_{eB}) with the volume fraction of homopolymer (f_C) for A_6B_6/C_2 blends in solutions with varying the concentration (Φ), where the interaction parameters are set as ε_{AB}=4.0, ε_{BC}=−4.0, ε_{AC}=2.0, ε_{AS}=−2.0, ε_{BS}=−2.0, ε_{CS}=−0.2.

ture, following the specific transition sequence: L → G/PL → C → S. By analogy, our research findings are thermodynamically rational: when Φ=0.4 and 0.5, the effective fraction f_{eB} first decreases from about 0.5 and then increases back to around 0.5, leading to the formation of a reentrant phase sequence with curvature first increasing and then decreasing; when Φ≥0.6, f_{eB} increases monotonically from about 0.5, driving the phase structure to transition solely toward the high-curvature direction.

Effects of Interaction Parameter and Block Length

In order to assess their effect on phase behavior, we varied the interaction parameters (ε_{BC}, ε_{BS}, ε_{AB}) and the copolymer chain length and present the phase diagrams and effective volume fractions in Figs. 4–6. We first investigated the phase behavior of A_6B_6/C_2 blends in solutions with fixed Φ=0.4 and interactions identical to those in Fig. 1(a) except for B-C interaction ε_{BC}, and plot the phase diagram in the f_C-ε_{BC} space (Fig. 4a). The B-C interaction ε_{BC} is varied from −6 to 0. As shown in Fig. 4(a), phase transitions including reentrant ones are observed when ε_{BC}≤ −4.0 and the f_C-window for inverted phases gets wider as $|\varepsilon_{BC}|$ increases. For example, upon increasing f_C, sequences L → PL/G(B+C) → C(B+C) → PL/G(B+C) → Dis and L → C(B+C) → PL/G(B+C) → L → Dis, are formed at ε_{BC}=−6.0 and ε_{BC}=−4.0, respectively. This is because a more negative ε_{BC} (stronger B-C attraction) drives solvent to preferentially swell A-domains over B+C-domains, reducing the effective volume fraction of B-domains and inducing inverted phases; with further increases in f_C, reentrant behavior emerges. When −4.0<ε_{BC}<0, the inverted phases and phase reentry phenomena are not observed, but only a partial sequence (L → G(A) → C(A) → S(A)) appears. When ε_{BC}=0, macrophase separation occurs even when a small amount of homopolymer is added. We also calculated the effective volume fraction f_{eB} as a function of f_C under the parameters in Fig. 4(a). In Fig. 4(b), it is noted that each f_{eB} curve presents a non-monotonic variation when ε_{BC}≤−4.0. This means that, with increasing f_C, each f_{eB} curve first decreases, reaches a minimum value, and then increases when ε_{BC}≤−4.0, which is consistent with the reentrant phase transitions shown in Fig. 4(a), indicating that the occurrence of reentrant phase transitions is caused by the non-monotonic variation of f_{eB}.

As shown in Fig. 5(a), we further systematically varied the B-solvent interaction ε_{BS} from −4 to 0 and fixed other parameters to be the same as those in Fig. 1(a). However, phase reentry phenomena do not occur when ε_{BS}≤−3.0 as shown in Fig. 5(a). In addition, the resulting phase sequence is L → G(A) → C(A) → S(A) when the attraction between B and solvent is strong (*i.e.*, ε_{BS}=−4.0). When ε_{BS}=−3.0, lamella is the major phase throughout the entire range of f_C, except the disorder phase at high f_C values. The inverted phases occur in a relatively wide f_C window when ε_{BS}≥−1.0, and reentrant phase transitions with the sequence PL/G(B+C) → C(B+C) → PL/G(B+C) → Dis occur when ε_{BS}=−1.0. However, no phase reentry phenomenon is observed, but only the sequence C(B+C)→Dis when ε_{BS}=−0.2. As shown in Fig. 5(b), the plot of f_{eB} versus f_C corresponds to the phase diagram in Fig. 5(a). When ε_{BS}≤−3.0, the system does not undergo inverted phases, and the values of f_{eB} are all greater than 0.5. When −1.0≤ ε_{BS}≤−2.0, the values of f_{eB} first decrease and then increase, indicating a phase reentrant phenomenon in the system. At ε_{BS}=−0.2, the system undergoes phase sequence of C(B+C)→Dis, and f_{eB} increases monotonically.

Fig. 6(a) shows the phase diagram of the A_6B_6/C_2 blends in solutions with ε_{AB} and f_C as parameters, where the ε_{AB} varies from 0 to 6 and Φ is fixed at 0.4. The other interaction parameters are the same as those in Fig. 1(a). Overall, the value of

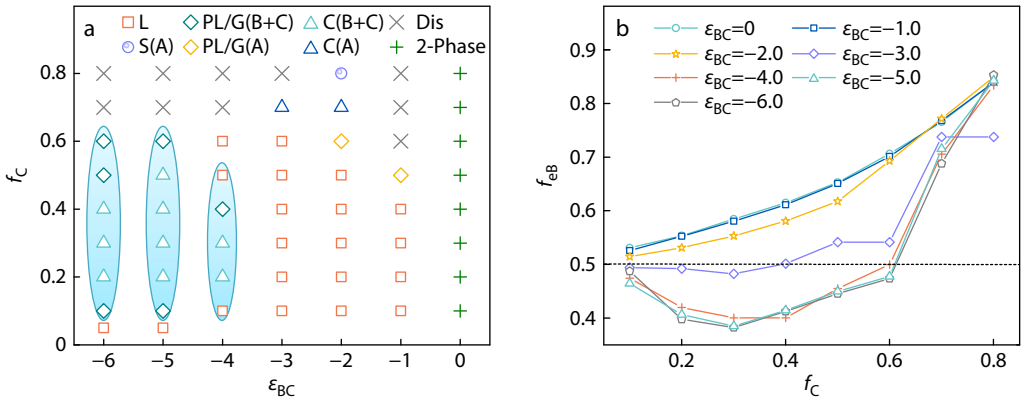

Fig. 4 (a) Phase diagrams for A_6B_6/C_2 blends in solutions with fixed polymer concentration Φ=0.4 in the volume fraction of homopolymer (f_C), and B-C interaction (ε_{BC}) space, with ε_{AB}=4.0, ε_{AC}=2.0, ε_{AS}=−2.0, ε_{BS}=−2.0, ε_{CS}=−0.2; (b) Variation of the effective volume fractions of B-domains (f_{eB}) with f_C. for A_6B_6/C_2 blends in solutions, under the same parameters corresponding to the phase diagrams in (a).

https://doi.org/10.1007/s10118-025-3546-9

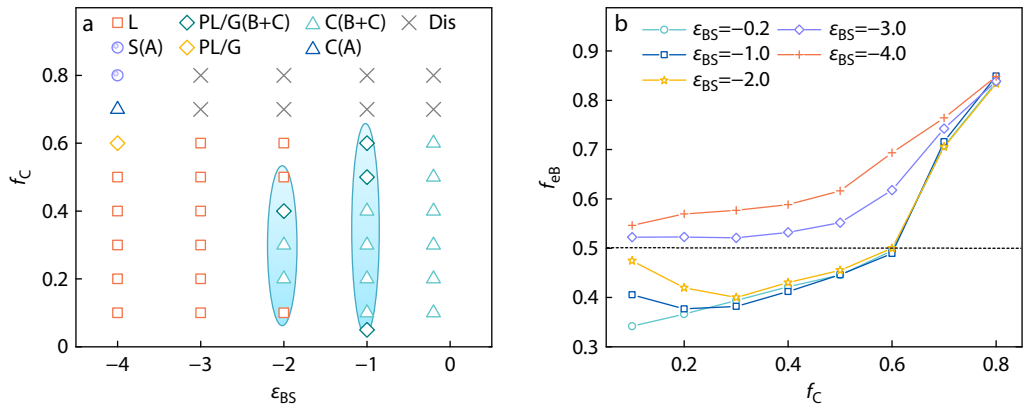

Fig. 5 (a) Phase diagrams for A_6B_6/C_2 blends in solutions with fixed polymer concentration Φ=0.4 in the volume fraction of homopolymer (f_C), and B-S interaction (ε_{BS}) space, with ε_{AB}=4.0, ε_{BC}=−4.0, ε_{AC}=2.0, ε_{AS}=−2.0, ε_{CS}=−0.2; (b) Variation of the effective volume fractions of B-domains (f_{eB}) with f_C for A_6B_6/C_2 blends in solutions, under the same parameters corresponding to the phase diagrams in (a).

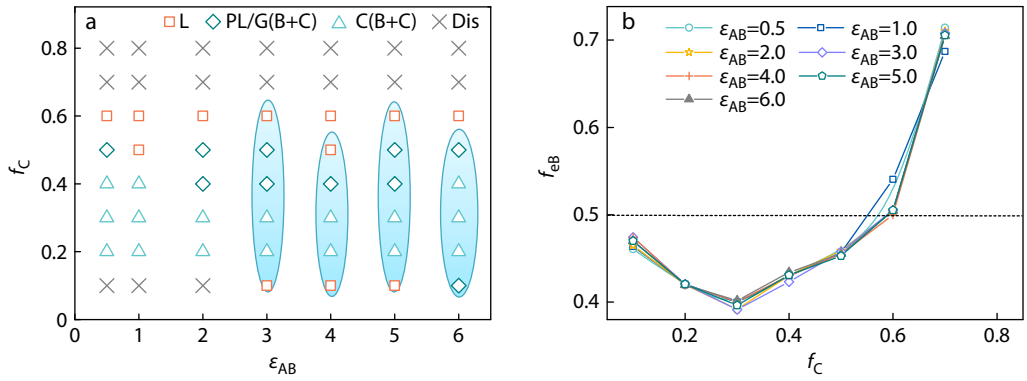

Fig. 6 (a) Phase diagrams for A_6B_6/C_2 blends in solutions with fixed polymer concentration Φ=0.4 in the volume fraction of homopolymer (f_C), and A-B interaction (ε_{AB}) space, with ε_{BC}=−4.0, ε_{AC}=2.0, ε_{AS}=−2.0, ε_{BS}=−2.0, ε_{CS}=−0.2; (b) Variation of the effective volume fractions of B-domains (f_{eB}) with f_C for A_6B_6/C_2 blends in solutions, under the same parameters corresponding to the phase diagrams in (a).

ε_{AB} has a relatively small effect on the phase structure of the system. When f_C=0.2–0.8, the phase sequence is the same for different values of ε_{AB}, which is C(B+C) → PL/G(B+C) → L → Dis, with slight differences in the f_C window of the phase. As shown in Fig. 6(b), system exhibits a phase reentrance phenomenon when ε_{AB}≥3, while no phase reentrance phenomenon is observed when ε_{AB}≤2. The main reason is that the phase structure is different when f_C=0.1. At f_C=0.1, the system forms a disordered structure when ε_{AB}≤2, while it forms a lamellar phase when 3<ε_{AB}<5. In Fig. 6(b), the f_{eB} curves show very little difference as the ε_{AB} varies; this corresponds to the observation that the self-assembly morphology does not change significantly with the change of ε_{AB}. Specifically, when ε_{AB}≤2.0, A- and B-blocks cannot be phase-separated, but the value of f_{eB} is roughly the same as that of forming the lamellar phase.

We also calculated the phase behavior of the asymmetric A_9B_3/C_2 blends in solution, comparing it with that of the symmetric A_6B_6/C_2 blends, and the phase diagram is shown in Fig. 7. This diagram shares identical parameters with Fig. 1, differing only in the lengths of the A-blocks and B-blocks. Comparing the asymmetric system with the symmetric system, a common point is that the value of f_{eB} increases with increasing Φ except the disordered phase. The difference lies in that the phase reentrance phenomenon observed in the symmetric system does not occur in the asymmetric system, and the f_{eB} curve increases monotonically with the increase of f_C. The different phase behaviors of these two systems are caused by the different volume fractions of blocks A and B. For asymmetric diblock copolymers A_9B_3, when no homopolymer is added, the volume fraction of B-blocks is small compared to that of the A-blocks. As the amount of homopolymer increases, the effective volume fraction of B increases. When there is less solvent, the phase behavior is similar to that of a melt, with a transition of PL/G(B+C) → L → C(B+C) → S occurring. When there is more solvent, the swelling effect of the solvent on A-domains is greater than that on B+C-domains, thus reducing the increase in the effective volume fraction of B. As a result, the lamellae appear at a larger f_C value in the system.

Solvent and Homopolymer Distribution

A significant window of lamellae was observed in our simulations as the homopolymer content increased. To understand the structural distribution of the homopolymer and solvent, we selected the system forming lamellae and disordered phase as examples, with ε_{AB}=4.0, ε_{AC}=2.0, ε_{BC}=−4.0, ε_{AS}=−2.0, ε_{BS}=−3.0, ε_{CS}=−0.2 (ε_{BS}=−3.0 in Fig. 5a). From the snapshots shown in Fig. 8, it is noted that homopolymer is distributed in the B-domains when f_C is small, and throughout the space when f_C is larger. We

https://doi.org/10.1007/s10118-025-3546-9

have observed the quantitative distributions of solvent molecules and homopolymer in phases obtained at f_C=0.3, 0.5, 0.8 from the density profile (ρ) curves shown in Fig. 9. Since there are only four species in our model systems, $\rho_A + \rho_B + \rho_C + \rho_S = 1$. In Figs. 9(a) and 9(b), the peaks of the ρ_B and ρ_C curves appear simultaneously, alternating with ρ_A, indicating that A-rich layers and B+C-rich layers alternate in the lamellae. The ρ_S value inside A-rich layers is higher than that inside B+C-rich layers. The maximum value of ρ_C is in accordance with the homopolymer volume fraction, f_C. Specifically, at f_C=0.3 (Fig. 9a), ρ_C ranges from 0 to 0.3, whereas at f_C=0.5 (Fig. 9b), this range extends to 0 to 0.5. However, it is noteworthy that the peaks of the ρ_A, ρ_B, and ρ_C curves in Fig. 9(b) exhibit less sharpness compared to those in Fig. 9(a), suggesting the presence of broader interfaces regions when f_C=0.5. This finding is corroborated by the snapshots presented in Figs. 8(c) and 8(e), demonstrating the consistency of our results. Further increases in the amount of homopolymer lead to the almost horizontal curves of ρ_A, ρ_B, ρ_C, and ρ_S in Fig. 9(c), corresponding to the disordered phase shown in Fig. 8(g). In this scenario, the density profile curves in

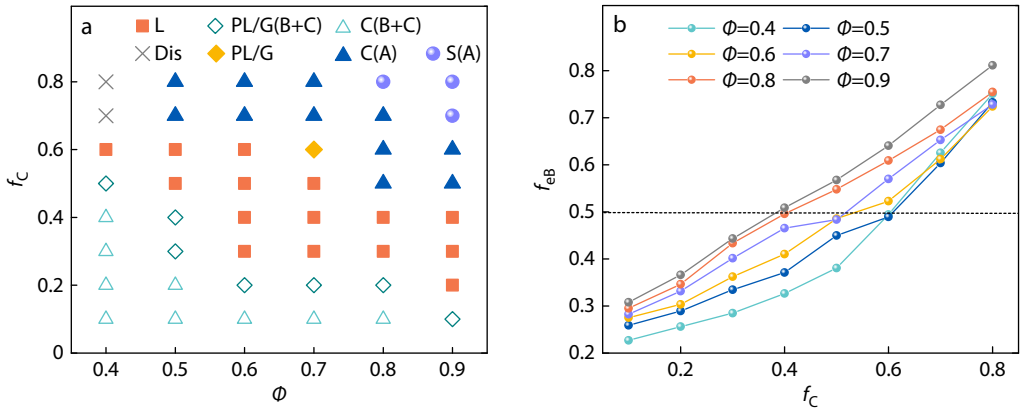

Fig. 7 (a) Phase diagram in the volume fraction of homopolymer (f_C), and the concentration (Φ) for A_9B_3/C_2 blends in solutions with f_C with ε_{AB}=4.0, ε_{BC}=−4.0, ε_{AC}=2.0, ε_{AS}=−2.0, ε_{BS}=−2.0, ε_{CS}=−0.2; (b) Variation of the effective volume fractions of B-domains (f_{eB}) with for A_9B_3/C_2 blends in solutions, under the same fixed interaction parameters as in (a).

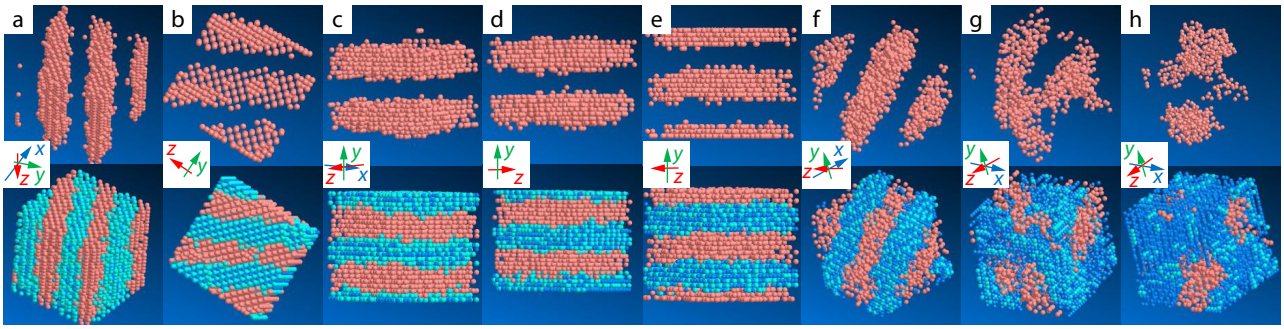

Fig. 8 Snapshots obtained with for A_6B_6/C_2 blends in solutions at Φ=0.4 with ε_{AB}=4.0, ε_{AC}=2.0, ε_{BC}=−4.0, ε_{AS}=−2.0, ε_{BS}=−3.0, ε_{CS}=−0.2, and with different homopolymer volume fractions (f_C). (a) f_C=0.1; (b) f_C=0.2; (c) f_C=0.3; (d) f_C=0.4; (e) f_C=0.5; (f) f_C=0.6; (g) f_C=0.7; (h) f_C=0.8. Phases: lamellar in snapshots (a–f), disordered in (g and h). Color scheme: A (red), B (green), C (blue). In the top row, only A-domains are shown for clarity.

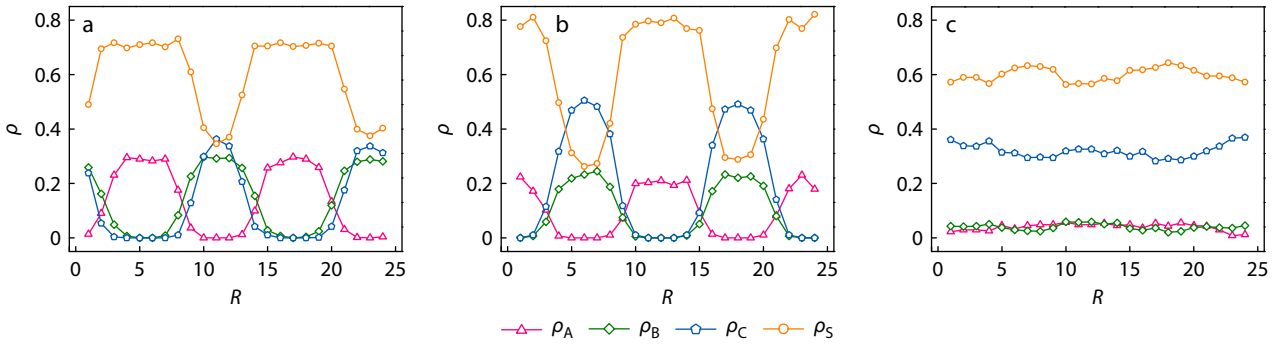

Fig. 9 Density profiles (ρ) of monomers and solvent in phases obtained from A_6B_6/C_2 blends in solutions at Φ=0.4 with ε_{AB}=4.0, ε_{AC}=2.0, ε_{BC}=−4.0, ε_{AS} =−2.0, ε_{BS}=−3.0, ε_{CS}=−0.2, with different different homopolymer volume fractions f_C. (a) f_C=0.3; (b) f_C=0.5; (c) f_C=0.8. For (a) and (b) (lamellar phases): the profile direction is normal to the lamellar layers. For (c) (disordered phase): The profile direction is an arbitrary axis direction. R is the distance to the reference layer. The volume of the simulation box is $V = 24 \times 24 \times 24$.

https://doi.org/10.1007/s10118-025-3546-9

any direction are identical, indicating that solvent molecules are almost uniformly distributed throughout the phase.

CONCLUSIONS

We systematically investigated the self-assembly of triple-hydrophilic diblock copolymer AB/homopolymer C blends in concentrated solutions using a simulated annealing method. We constructed phase diagrams of the system by varying the polymer concentration and volume fraction of homopolymer. For a given polymer concentration Φ, we observed rich phase transition sequences with increasing homopolymer volume fraction f_C, especially reentrant phase transitions, such as lamellae → inverted cylinders → gyroids → lamellae → disorder. By analyzing the variations in the average contact numbers, as well as the effective volume fractions of domains, we elucidated the mechanism of reentrant phase transitions. We found that at low polymer concentrations, the phase behavior depends on both homopolymer addition and solvent selectivity. The combined effect of solvent selectivity and interaction with homopolymer can be used to tune the degree of swelling of the two blocks, resulting in a nonmonotonic variation of the effective volume fraction of the A (or B)- domains with the increase of f_C, and further induce the reentrant phase transitions. In contrast, at high polymer concentrations, B-C attractions dominate, while the solvent's influence is relatively weak. Consequently, the effective volume fraction of B-domains increases monotonically with increasing f_C, and no reentrant phase transitions occur. To assess the effect of key parameters on phase behavior, we varied the interaction parameters (ε_{BC}, ε_{BS}, ε_{AB}) and the copolymer chain length, and presented the corresponding phase diagrams and effective volume fractions. Our findings include: (1) reentrant phase transitions are only observed when ε_{BC} decreases (*i.e.*, becomes more negative), and the inverted phases f_C-window gets wider as ε_{BC} decreases. This is because a more negative ε_{BC} (stronger B-C attraction) drives solvent to preferentially swell A-domains over B+C-domains, reducing the effective volume fraction of B-domains and inducing inverted phases; with further increases in f_C, reentrant behavior emerges; (2) increasing ε_{BS} (weakening B-solvent attraction) has a similar effect to decreasing ε_{BC}. However, when ε_{BS}=−0.2, reentrant behavior disappears—even with more homopolymer swelling B-domains, the volume fraction of B-domains cannot compete with that of A-domains, so only inverted phases form. (3) ε_{AB} has a relatively small effect on the phase structure of the system. (4) For asymmetric diblock copolymers A_9B_3, no reentrant behavior is observed: at high concentrations, the phase behavior resembles that of a melt, with a transition of PL/G(B+C) → L → C(B+C) → S; at low concentrations, the swelling effect of the solvent on A is greater than that on B+C, thus reducing the increase in the effective volume fraction of B, the lamellae appear at a larger f_C value in the system. These results enhance understanding of the self-assembly mechanism of AB/C blends in concentrated solutions. They also provide guidance for the preparation of blended materials, facilitating the screening of suitable components, volume fractions of each component, and other key parameters.

Conflict of Interests

The authors declare no interest conflict.

Electronic Supplementary Information

Electronic supplementary information (ESI) is available free of charge in the online version of this article at http://doi.org/10.1007/s10118-025-3546-9.

Data Availability Statement

The data supporting the findings of this study are available from the corresponding author upon reasonable request.

ACKNOWLEDGMENTS

This study was financially supported by the Natural Science Foundation of Shandong Province (Nos. ZR2023QA136, ZR2021MA073 and ZR2024QA235) and the National Natural Science Foundation of China (No. 22173051).

REFERENCES

1 Doerk, G. S.; Kulkarni, A. A.; Li, R. Engineering self-assembled domain asymmetry in solvent vapor annealed block copolymer-homopolymer blend films. *Macromolecules* **2024**, *57*, 181−190.
2 Maekawa, S.; Seshimo, T.; Dazai, T.; Sato, K.; Sato, K. H.; Nabae, Y.; Hayakawa, T. Chemically tailored block copolymers for highly reliable sub-10-nm patterns by directed self-assembly. *Nat. Commun.* **2024**, *15*, 1−11.
3 Polymeropoulos, G.; Zapsas, G.; Ntetsikas, K.; Bilalis, P.; Gnanou, Y.; Hadjichristidis, N. 50th Anniversary perspective: polymers with complex architectures. *Macromolecules* **2017**, *50*, 1253−1290.
4 Zhang, W. J.; Hong, C. Y.; Pan, C. Y. Polymerization-induced self-assembly of functionalized block copolymer nanoparticles and their application in drug delivery, *Macromol. Rapid Commun.* **2018**, 1800279.
5 Parkin, H. C.; Street, S. T. G.; Gowen, B.; Da-Silva-Correa, L. H.; Hof, R.; Buckley, H. L.; Manners, I. Mechanism of action and design of potent antibacterial block copolymer nanoparticles. *J. Am. Chem. Soc.* **2024**, *146*, 5128−5141.
6 Hur, Y. H.; Song, S. W.; Kim, J. M.; Park, W. I.; Kim, K. H.; Kim, Y. J.; Jung, Y. S. Thermodynamic and kinetic tuning of block copolymer based on random copolymerization for high-quality sub-6 nm pattern formation. *Adv. Funct. Mater.* **2018**, 1800765.
7 Tao, Y. X.; Chen, L. L.; Liu, Y. H.; Hu, X.; Zhu, Z.; Guo, K. Synthesis and self-assembly of silicon-containing block copolymers for sub 5 nm nanolithography. *Acta Polymerica Sinica* (in Chinese) **2022**, *53*, 1445−1458.
8 Su, G.; Zhang, Z.; Xiao, M.; Wang, S.; Huang, S.; Guo, H.; Han, D.; Meng, Y. Boosting electrochemical performance by regulating rigid-flexible microphase separation of multiblock copolymers. *Chem. Eng. J.* **2024**, *500*, 157050.
9 Wang, T.; Zhong, L.; Xiao, M.; Han, D.; Wang, S.; Huang, Z.; Huang, S.; Sun, L.; Meng, Y. Block copolymer electrolytes for lithium metal batteries: strategies to boost both ionic conductivity and mechanical strength. *Prog. Polym. Sci.* **2023**, *146*, 101743.
10 Moirangthem, P. M.; Shagolsem, L. S. Phase and order behavior of charged asymmetric diblock-copolymer melts in bulk. *Macromol.*

Graphical Abstract

Reentrant Phase Behavior in Diblock Copolymer AB/Homopolymer C Blends: A Combined Effect of Solvent Selectivity and Block Interactions

Zhi-Yao Liu, Hui Wang, Hong-Xia Bu, Juan Wang, Bao-Hui Li, and Lu-Lu Liu

Qilu Normal University; Nankai University; Shandong Jianzhu University

The phase behavior of diblock copolymer AB/homopolymer C blends in concentrated aqueous solutions was investigated using a simulated annealing method. The studies reveal reentrant phase behavior in the system with increasing homopolymer content, driven by the competing swelling effects of the solvent and homopolymer.

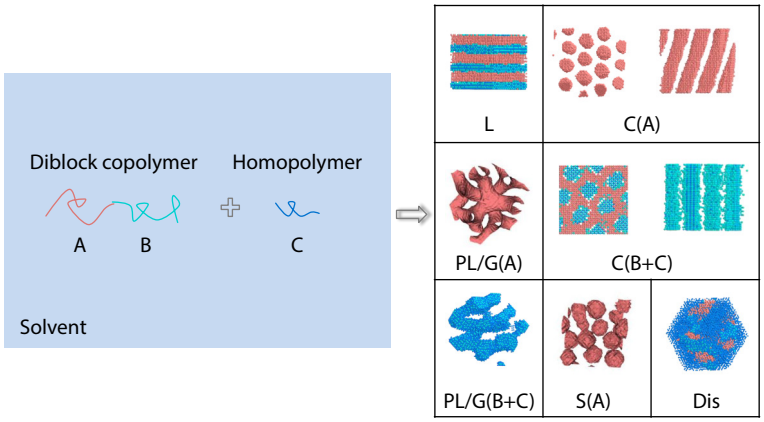

Chinese J. Polym. Sci. 2026, 44, 857–868 *https://doi.org/10.1007/s10118-025-3546-9*

Symp. **2024**, *413*, 2300028.
11 Masten, M. W.; Schick, M. Stable and unstable phase in diblock copolymer melt. *Phys. Rev. Lett.* **1994**, *72*, 2660–2663.
12 Beardsley, T. M.; Matsen, M. W. Monte carlo phase diagram for diblock copolymer melts. *Eur. Phys. J. E.* **2010**, *32*, 255–264.
13 Matsen, M. W. Effect of architecture on the phase behavior of AB-type block copolymer melts. *Macromolecules* **2012**, *45*, 2161–2165.
14 Chen, H.; Dong, Q.; Qiang, Y.; Peng, L.; Huang, X.; Li, W. Mechanisms of multiple reentrant transitions between Frank-Kasper and classical spherical phases in AB-type dendron-like copolymer. *Macromolecules* **2025**, *58*, 10192–10202.
15 Shi, W.; Li, W.; Delaney, K. T.; Fredrickson, G. H.; Kramer, E. J.; Ntaras, C.; Avgeropoulos, A.; Lynd, N. A. Morphology re-entry in asymmetric PS-PI-PS′ triblock copolymer and PS homopolymer blends. *J. Polym. Sci., Part B: Polym. Phys.* **2016**, *54*, 169–179.
16 Chen, L.; Qiang, Y.; Li, W. Tuning arm architecture leads to unusual phase behaviors in a $(BAB)_5$ star copolymer melt. *Macromolecules* **2018**, *51*, 9890–9900.
17 Peng, Z.; Ghasemi, M.; Michels, J. J.; Ade, H. Re-entrant phase behaviour of organic semiconductors. *Nat. Mater.* **2025**, *24*, 1785–1792.
18 Liu, J.; Jiang, Y.; Liu, R.; Jin, J.; Wei, S.; Ji, W.; He, X.; Wu, F.; Yu, P.; Mao, L. Vitamin C drives reentrant actin phase transition: biphasic exocytosis regulation revealed by single-vesicle electrochemistry. *J. Am. Chem. Soc.* **2024**, *146*, 17747–17756.
19 Su, L.; Mosquera, J.; Mabesoone, M. F. J.; Schoenmakers, S. M. C.; Muller, C.; Vleugels, M. E. J.; Dhiman, S.; Wijker, S.; Palmans, A. R. A.; Meijer, E. W. Dilution-induced gel-sol-gel-sol transitions by competitive supramolecular pathways in water. *Science* **2022**, *377*, 213–218.
20 Pegoraro, C.; Karpova, E.; Qutbuddin, Y.; Sanchis, E. M.; Dimitrijevs, P.; Huck-Iriart, C.; Gavrilović, S.; Arsenyan, P.; Schwille, P.; Felip-León, C.; Duro-Castano, A.; Conejos-Sanchez, I.; Vicent, M. J. Polyproline-polyornithine diblock copolymers with inherent mitochondria tropism. *Adv. Mater.* **2025**, 2411595.
21 Chrysostomou, V.; Da Vela, S.; Pispas, S.; Papadakis, C. M. PH and temperature dependence of low-core tg micellar structures formed by PDMAEMA-*b*-PLMA diblock copolymers in aqueous solution. *J. Polym. Sci.* **2025**, *63*, 1684–1694.
22 Constantin, M.; Ailiesei, G.; Fundueanu, G.; Tarabukina, E.; Krasova, A.; Filippov, A. Synthesis and behavior in aqueous solution of carboxymethyl pullulan-graft-poly(*N*-isopropylacrylamide-*co*-methacrylamide). *J. Mol. Liq.* **2024**, *399*, 124338.
23 Bednarek, M.; Grabowski, M. Polylactide/poly(vinyl monomer) block copolymers for specific applications. *Polym. Rev.* **2024**, 2310105.
24 Yokota, K.; Usuda, S.; Nishimura, T.; Takahashi, R.; Taoka, Y.; Kobayashi, S.; Tanaka, M.; Matsumura, K.; Yusa, S. I. Self-assembly and drug encapsulation properties of biocompatible amphiphilic diblock copolymers. *Langmuir* **2025**, *41*, 765–773.
25 Han, Y.; Lu, Y.; Song, T.; Cui, J.; Fan, J. Topology-directed coassembly of linear and cyclic amphiphilic diblock copolymers: a Monte Carlo study. *Langmuir* **2024**, *40*, 16103–16112.
26 Pavlenko, S. A.; Larin, D. E.; Govorun, E. N. Self-assembly of

hydrophobic-amphiphilic diblock copolymers in solution. *J. Phys. Condens. Matter.* **2022**, *34*, 125001.
27 Fischer, J.; Porcar, L.; Cabral, J. T.; Sottmann, T. Using an amphiphilic diblock copolymer to understand the shear-induced structural transformation of bicontinuous microemulsions. *J. Colloid Interface Sci.* **2024**, *671*, 124–133.
28 Yokota, K.; Takahashi, R.; Ngan, V. T.; Nishimura, T.; Kappl, M.; Fujii, S.; Yusa, S. I. Preparation of water-soluble polyion complex (pic) micelles with pH-responsive carboxybetaine block. *Macromol. Rapid Commun*. **2024**, 2400532.
29 Higaki, Y.; Toyama, H.; Masuda, T.; Kobayashi, S.; Tanaka, M. Microphase separation of double-hydrophilic poly(carboxybetaine acrylate)-poly(2-methoxyethyl acrylate) block copolymers in water. *Polym. J.* **2023**, *55*, 1357–1365.
30 Wu, R.; Yan, Y.; Li, X.; Tan, Y. Preparation and evaluation of double-hydrophilic diblock copolymer as viscosity reducers for heavy oil. *J. Appl. Polym. Sci.* **2023**, *140*, e53278.
31 Blanazs, A.; Warren, N. J.; Lewis, A. L.; Armes, S. P.; Ryan, A. J. Self-assembly of double hydrophilic block copolymers in concentrated aqueous solution. *Soft Matter* **2011**, *7*, 6399–6403.
32 Casse, O.; Shkilnyy, A.; Linders, J.; Mayer, C.; Häussinger, D.; Völkel, A.; Thünemann, A. F.; Dimova, R.; Cölfen, H.; Meier, W.; Schlaad, H.; Taubert, A. Solution behavior of double-hydrophilic block copolymers in dilute aqueous solution. *Macromolecules* **2012**, *45*, 4772–4777.
33 Wu, J. P.; Wang, Z.; Yin, Y. H.; Jiang, R.; Li, B. H. A simulation study of phase behavior of double-hydrophilic block copolymers in aqueous solutions. *Macromolecules* **2015**, *48*, 8897–8906.
34 Xie, J. Y.; Lai, C. T.; Shi, A. C. Regulating the self-assembly of AB/CD diblock copolymer blends via secondary interactions. *J. Polym. Sci.* **2024**, *62*, 716–732.
35 Toth, K.; Bae, S.; Osuji, C. O.; Yager, K. G.; Doerk, G. S. Film thickness and composition effects in symmetric ternary block copolymer/homopolymer blend films: domain spacing and orientation. *Macromolecules* **2021**, *54*, 7970–7986.
36 Bezik, C. T.; Mysona, J. A.; Schneider, L.; Ramírez-Hernández, A.; Müller, M.; de Pablo, J. J. Is the "bricks-and-mortar" mesophase bicontinuous? Dynamic simulations of miktoarm block copolymer/homopolymer blends. *Macromolecules* **2022**, *55*, 745–758.
37 Hong, S. J.; Kim, G. R.; Kim, N. K.; Shin, J.; Kim, Y. W. Poly(amide11)-incorporated block copolymers as compatibilizers to toughen a poly(lactide)/polyamide 11 blend. *ACS Appl. Polym. Mater.* **2024**, *6*, 1224–1235.
38 Dobrosielska, K.; Wakao, S.; Suzuki, J.; Noda, K.; Takano, A.; Matsushita, Y. Effect of homopolymer molecular weight on nanophase-separated structures of AB block copolymer/C homopolymer blends with hydrogen-bonding interactions. *Macromolecules* **2009**, *42*, 7098–7102.
39 Matsushita, Y. Creation of hierarchically ordered nanophase structures in block polymers having various competing interactions. *Macromolecules* **2007**, *40*, 771–776.
40 Dobrosielska, K.; Wakao, S.; Takano, A.; Matsushita, Y. Nanophase-separated structures of AB block copolymer/C homopolymer blends with complementary hydrogen-bonding interactions. *Macromolecules* **2008**, *41*, 7695–7698.
41 Dehghan, A.; Shi, A. C. Modeling hydrogen bonding in diblock copolymer/homopolymer blends. *Macromolecules* **2013**, **46**, 5796–5805.
42 Hameed, N.; Guo, Q. Nanostructure and hydrogen bonding in interpolyelectrolyte complexes of poly(ε-caprolactone)-block-poly(2-vinyl pyridine) and poly(acrylic acid). *Polymer* **2008**, *49*, 5268–5275.
43 Hameed, N.; Liu, J.; Guo, Q. Self-assembled complexes of poly(4-vinylphenol) and poly(ε-caprolactone)-block-poly(2-vinylpyridine) *via* competitive hydrogen bonding. *Macromolecules* **2008**, *41*, 7596–7605.
44 Hameed, N.; Guo, Q. Selective hydrogen bonding and hierarchical nanostructures in poly(hydroxyether of bisphenol A)/poly(ε-caprolactone)-block-poly(2-vinyl pyridine) blends. *Polymer* **2008**, *49*, 922–933.
45 Salim, N. V.; Hanley, T.; Guo, Q. Microphase separation through competitive hydrogen bonding in double crystalline diblock copolymer/homopolymer blends. *Macromolecules* **2010**, *43*, 7695–7704.
46 Li, J. G.; Lin, Y. D.; Kuo, S. W. From microphase separation to self-organized mesoporous phenolic resin through competitive hydrogen bonding with double-crystalline diblock copolymers of poly(ethylene oxide-*b*-ε-caprolactone). *Macromolecules* **2011**, *44*, 9295–9309.
47 Salim, N. V.; Hameed, N.; Guo, Q. Competitive hydrogen bonding and self-assembly in poly(2-vinyl pyridine)-block-poly(methyl methacrylate)/poly(hydroxyether of bisphenol A) blends. *J. Polym. Sci., Part B: Polym. Phys.* **2009**, *47*, 1894–1905.
48 Hameed, N.; Salim, N. V.; Guo, Q. Microphase separation through competitive hydrogen bonding in self-assembled diblock copolymer/homopolymer complexes. *J. Chem. Phys.* **2009**, *131*, 214905.
49 Chen, S. C.; Kuo, S. W.; Jeng, U. S.; Su, C. J.; Chang, F. C. On modulating the phase behavior of block copolymer/homopolymer blends *via* hydrogen bonding. *Macromolecules* **2010**, *43*, 1083–1092.
50 Xia, B.; Li, W.; Qiu, F. Self-assembling behaviors of symmetric diblock copolymers in C homopolymers. *Acta Chim. Sin.* **2014**, *72*, 30–34.
51 Qiu, H.; Oliver, A. M.; Gwyther, J.; Cai, J.; Harniman, R. L.; Hayward, D. W.; Manners, I. Uniform toroidal micelles via the solution self-assembly of block copolymer-homopolymer blends using a "frustrated crystallization" approach. *Macromolecules* **2019**, *52*, 113–120.
52 Liu, J. Y.; Song, H. R.; Wang, M.; Jin, S. H.; Liang, Z.; Mao, X.; Li, W.; Deng, R. H.; Zhu, J. T. Asymmetric mesoporous carbon microparticles by 3D-confined self-assembly of block copolymer/homopolymer blends and selective carbonization. *Chinese J. Polym. Sci.* **2023**, *41*, 787–793.
53 Liu, Z. Y.; Wang, Z.; Yin, Y. H.; Jiang, R.; Li, B. H. A simulation study of enhancing the compatibility in block copolymer AB/homopolymer C blends by solvents. *Acta Polymerica Sinica* (in Chinese) **2019**, *50*, 1220–1228.
54 Tan, J. Y.; Liu, Z. Y.; Wang, R.; Zhou, Y.; Xie, S. Y.; Li, B. H.; Wan, X. H.; Zhang, J. Modulation of thermodynamic and kinetic inverted phase behavior of block copolymers by inorganic polyoxometalates. *Soft Matter* **2019**, *15*, 6988–6993.
55 Zheng, X. H.; Ren, M.; Wang, H.; Wang, H. Y.; Geng, Z.; Xu, J. P.; Deng, R. H.; Chen, S. B.; Binder, W. H.; Zhu, J. T. Halogen-bond mediated 3D confined assembly of AB diblock copolymer and C homopolymer blends. *Small* **2021**, *17*, 1–10.
56 Carmesin, I.; Kremer, K. The bond fluctuation method: a new effective algorithm for the dynamics of polymers in all spatial dimensions. *Macromolecules* **1988**, *21*, 2819–2823.
57 Larson, R. G. Monte Carlo simulation of micro-structural transitions in surfactant systems. *J. Chem. Phys.* **1992**, *96*, 7904–7918.
58 Grest, G. S.; Soukoulis, C. M.; Levin, K. Cooling-rate dependence

for the spin-glass ground-state energy: implications for optimization by simulated annealing. *Phys. Rev. Lett.* **1986**, *56*, 1148–1151.
59 Wu, J.; Wang, X.; Wang, Z.; Yin, Y.; Jiang, R.; Li, Y.; Li, B. Nanospheres with patches arranged in polyhedrons from self-assembly of solution-state diblock copolymers under spherical confinement. *Macromolecules* **2023**, *56*, 335–348.
60 Li, X. Y.; Wang, Z.; Yin, Y. H.; Jiang, R.; Li, B. H. Interfacial frustration-induced novel self-assembled structures from block copolymers under janus spherical confinement. *Chinese J. Polym. Sci.* **2025**, *43*, 1423–1432.
61 Sun, P.; Yin, Y.; Li, B.; Chen, T.; Jin, Q.; Ding, D.; Shi, A. C. Simulated annealing study of gyroid formation in diblock copolymer solutions. *Phys. Rev. E* **2005**, *72*, 061408.
62 Zhang, J.; Kong, W.; Duan, H. Soft confinement-induced morphologies of the blends of AB diblock copolymers and C homopolymers. *Langmuir* **2017**, *33*, 3123–3133.
63 Zheng, L. F.; Wang, Z.; Yin, Y. H.; Jiang, R.; Li, B. H. Monte carlo simulations of the self-assembly of ABA triblock copolymers inside an oil-in-water emulsion droplet. *Acta Polymerica Sinica* (in Chinese) **2019**, *50*, 915–924.
64 Wu, J.; Wang, Z.; Yin, Y.; Jiang, R.; Li, B. Phase behavior of ABC cyclic terpolymer melts: a simulation study. *Soft Matter* **2020**, *16*, 2706–2714.
65 Zheng, L.; Wu, J.; Wang, Z.; Yin, Y.; Jiang, R.; Li, B. Phase behavior of ABC-type triple-hydrophilic block copolymers in aqueous solutions. *Eur. Phys. J. E.* **2016**, *39*, 75.
66 Li, Q.; Woo, D.; Kim, J. K.; Li, W. Truly "inverted" cylinders and spheres formed in the $A(AB)_3$/AC blends of B/C hydrogen bonding interactions. *Macromolecules* **2022**, *55*, 6525–6535.

https://doi.org/10.1007/s10118-025-3546-9